ELSEVIER

Journal of Power Sources 68 (1997) 501–505

JOURNAL OF POWER SOURCES

In situ scanning vibrating electrode technique for lithium metal anodes

Masashi Ishikawa [a,*], Masayuki Morita [a], Yoshiharu Matsuda [b]

[a] Department of Applied Chemistry and Chemical Engineering, Faculty of Engineering, Yamaguchi University, 2557 Tokiwadai, Ube 755, Japan

[b] Department of Applied Chemistry, Faculty of Engineering, Kansai University, 3-3-35 Yamate-cho, Suita 564, Japan

Accepted 27 December 1996

Abstract

The effect of the inorganic additives to electrolytes, aluminum iodide (AlI_3) and tin(II) iodide, on the charge/discharge coulombic efficiency of a lithium (Li) metal anode has been investigated in binary solvent systems, i.e., propylene carbonate (PC) mixed with 2-methyltetrahydrofuran (2Me-THF) containing lithium perchlorate ($LiClO_4$), PC + 2Me-THF/$LiClO_4$, and PC mixed with 1,2-dimethoxyethane (DME) containing $LiClO_4$, PC + DME/$LiClO_4$. AlI_3 improved the coulombic efficiency of the Li metal anode in both the binary solvent systems. Two-dimensional Li ionic currents at the interface of the Li metal anode were monitored by using in situ scanning vibrating electrode technique (SVET) in the representative binary system, PC + 2Me-THF/$LiClO_4$, in the absence and presence of the additives. The relationship between the coulombic efficiency and the Li ionic current distribution on the anode was discussed. © 1997 Published by Elsevier Science S.A.

Keywords. Rechargeable lithium batteries; Lithium metal anodes; Coulombic efficiency

1. Introduction

It is widely known that the characteristics of the interface between a lithium (Li) metal electrode and an organic electrolyte are much correlated with the charge/discharge performance of the Li metal electrode. Among various chemical and physical analysis, an in situ a.c. impedance method is a popular and informative tool for the elucidation of electrochemical characteristics of the Li electrode interface [1–4]. However, little is known about in situ methods which can detect the dynamic behavior of ionic currents at the electrode interface during a charge/discharge process, while in situ X-ray photospectroscopy (XPS) and Fourier-transform infrared (FT-IR) analysis offer clear information on the chemical composition of the Li electrode surface [2,5,6].

Recently, we proposed in situ scanning vibrating electrode technique (in situ SVET) as a novel and powerful tool for the observation of the Li ionic current distribution on the Li electrode surface during the discharge of the Li electrode in the single solvent system, PC/$LiClO_4$ [4,7]. Applied SVET system can detect the two-dimensional distribution of Li ionic currents on the tested electrode surface. The in situ SVET revealed the magnitude and distribution of the Li ionic currents on the anode substrate in the absence and presence of additives to the electrolyte, e.g., aluminum iodide [4,7]. The variation in uniformity and magnitude of the Li ionic currents observed by SVET on the anode substrate correlated well with the variation in the coulombic efficiency of charge/discharge cycling of Li on the substrate [4,7]. We report herein the effect of the electrolyte additives on the coulombic efficiency of the Li anode and on the distribution of Li ionic currents at the Li anode interface in practical electrolyte systems, i.e., propylene carbonate (PC) mixed with 2-methyltetrahydrofuran (2Me-THF) containing lithium perchlorate ($LiClO_4$), PC + 2Me-THF/$LiClO_4$, and PC mixed with 1,2-dimethoxyethane (DME) containing $LiClO_4$, PC + DME/$LiClO_4$ as binary solvent systems. In order to observe the Li ionic currents at the Li anode in the present electrolyte systems, we applied a new version of the in situ SVET system which improved in its resolving power. The dimensional resolution of the new SVET system is about 10 μm (maximum 2 μm), while the resolution of our previous SVET system [2,7] was about 0.3 mm.

2. Experimental

The solvents, PC, 2Me-THF, and DME (Mitsubishi Chemical, battery grade), were used as received. The electrolytes used were 1 mol dm^{-3} solutions of $LiClO_4$ (Ishizu Phar-

* Corresponding author

PII S0378-7753(97)02524-X

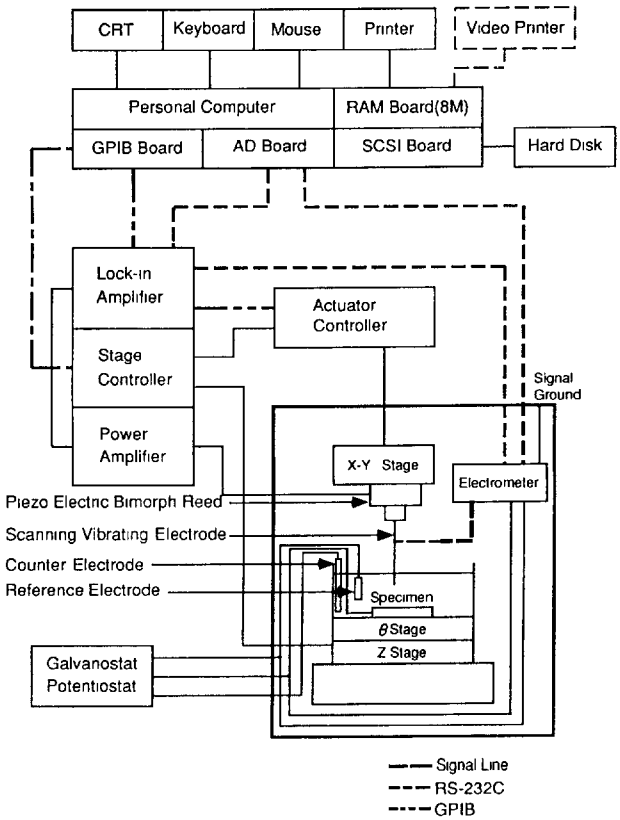

Fig. 1. Scheme of the scanning vibrating electrode instrumentation.

maceutical, extra pure grade) dissolved in a 1:1 mixture by volume of PC with 2Me-THF or DME: these binary electrolytes are expressed as PC + 2Me-THF/$LiClO_4$ and PC + DME/$LiClO_4$, respectively (see Introduction). The additives were aluminum iodide (AlI_3) and tin(II) iodide (SnI_2) and were used after dehydration with conventional methods. The conventional beaker-type glass cell with three electrodes was used for charge/discharge cycling test. The test electrode was a nickel (Ni) disk, whose surface area exposed to the electrolyte solution was 0.95 cm^2. The counter and the reference electrodes consisted of an Li sheet ($\sim$25 cm^2) and an Li chip (Li/Li^+), respectively. The coulombic efficiency in the charge/discharge cycle of Li was determined by a galvanostatic deposition/dissolution technique using an Ni disk substrate. The current density for cycling was 2.0 mA cm^{-2}, and the charged electricity was 0.2 C cm^{-2}. The cutoff voltage for the discharge of the test electrode was 1.5 V versus Li/Li^+.

The SVET system (Hokuto Denko, HV-301) was modified for Li battery systems. This improved SVET can offer potential gradient profiles induced by the Li ionic currents on the surface of the Li-deposited electrode during the discharge. Fig. 1 represents the outline of the in situ SVET system. The scanning vibrating (SV) electrode (a Pt wire electrode) attached to a sensor probe was vibrated (625 Hz) along a vertical axis (z-direction) in the vicinity of the test specimen electrode surface (distance between the SV electrode and the test electrode was 2–50 μm) by a piezoelectric oscillator. In our system the test specimen electrode (Ni plate: 1.0 cm^2) was laid on the bottom of the test cell. We obtained a potential gradient value, which is the difference between the potential detected by the SV electrode at the highest position and that at the lowest position during the vertical vibration of the SV electrode. The distance between the highest and the lowest positions was 0.6 μm. Therefore, the potential gradient values correspond to the potential gaps between a distance of 0.6 μm along the vertical axis in the vicinity of the test electrode surface. This potential gradient is proportional to the ionic current in the vicinity of the electrolyte–test electrode interface because the resistance of each electrolytes can be regarded as a constant. Thus, the potential gradient increases with an increase in ionic current. The x–y stage, on which the SV electrode was mounted, was moved horizontally by a stepping motor, while the test cell with the test electrode was fixed. By gathering the potential gradient values at various x–y positions, a two-dimensional potential gradient map on the test electrode could be obtained. The side of the wire-shaped (column-shaped) SV electrode was coated with thin glass layer, and only the bottom of the SV electrode was exposed to the electrolytes. In other words, only the exposed bottom was sensible to the ionic currents. Therefore, the dimensional resolving power of the SV electrode was directly correlated with the diameter of the SV electrode bottom. The diameter of the SV electrodes used was 2–50 μm (typically 10 μm in the present study). Thus, the apparent dimensional resolving power of the SVET system is 2–50 μm (typically 10 μm in the present study). In addition, a potentiostat/galvanostat was used to charge and discharge Li on the test electrode. The counter and the reference electrodes were an Li sheet (11.3 cm^2) and a small Li chip (Li/Li^+), respectively. Actual configuration and shape of test, counter, and reference electrodes in the test cell are shown in Fig. 2. All electrochemical measurements were carried out under an argon atmosphere at room temperature (20–25 °C).

3. Results and discussion

Fig. 3 shows coulombic efficiency for charge/discharge cycling of Li in PC + 2Me-THF/$LiClO_4$ (1 mol dm^{-3}) solutions in the absence and presence of AlI_3 at a constant charge/discharge current density of 2.0 mA cm^{-2}. The charged electricity was 0.2 C cm^{-2}, and the rest time between discharging and charging was 50 s. The effect of the addition of AlI_3 on the coulombic efficiency was clearly observed with an increase in AlI_3 concentration (100–500 ppm). On the other hand, no obvious improvement in cycling efficiency was observed for the corresponding solvent system with SnI_2 (100–200 ppm) as shown in Fig. 4: the charge/discharge condition in Fig. 4 (and also Figs. 5 and 6) was identical with that in Fig. 3. The effect of the additives, AlI_3 and SnI_2, was also investigated in another electrolyte, PC + DME/$LiClO_4$. Fig. 5 displays the coulombic efficiency in PC + DME/$LiClO_4$ (1 mol dm^{-3}) in the absence and presence of AlI_3.

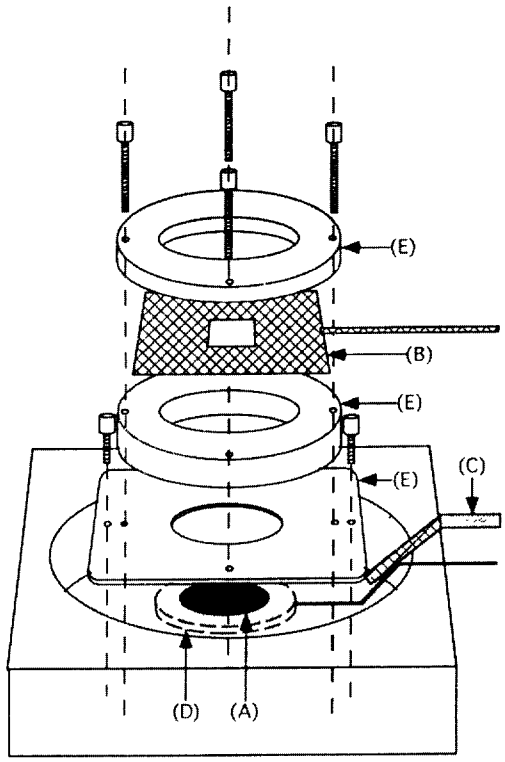

Fig 2 Schematic diagram of test cell for SVET, (A) test electrode; (B) counter electrode (Li with Ni mesh), (C) reference electrode (Li with Ni mesh), (D) current collector (Ni plate); (E) Teflon spacer.

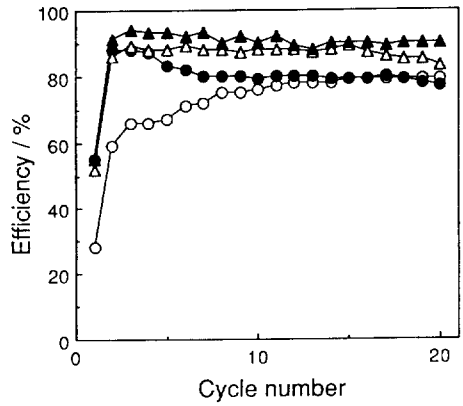

Fig 3 Effect of the addition of AlI_3 on the charge/discharge coulombic efficiency of Li in PC + 2Me-THF/$LiClO_4$, current density: 2.0 mA cm $^{-2}$; charged electricity 0.2 C cm^{-2}, (○) no additive; (●) AlI_3: 100 ppm; (△) AlI_3: 200 ppm; (▲) AlI_3 500 ppm

The addition of AlI_3 induced an increase in coulombic efficiency, while the effective concentration of AlI_3 was lower (100 ppm) in the PC+DME system than that in the PC + 2Me-THF system (500 ppm: Fig. 3). In analogy with the result in the PC + 2Me-THF system with SnI_2, no obvious improvement of the cycling efficiency was observed for the PC + DME system with SnI_2 (100–200 ppm) as shown in Fig. 6.

Both Sn and Al are well known to form Li alloys [4,8]. The thin layers of the Li alloys at the electrode surface during cathodic deposition of Li suppress the dendritic deposition of Li which causes the lowering of the coulombic efficiencies [4,8]. Our previous study suggests that Al forms the Li alloy films with high conductivity at the electrode surface, while the addition of SnI_2 causes a higher resistance than that of

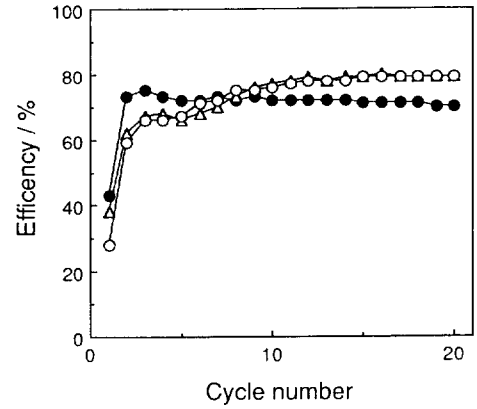

Fig. 4. Effect of the addition of SnI_2 on the charge/discharge coulombic efficiency of Li in PC + 2Me-THF/$LiClO_4$; current density: 2.0 mA cm^{-2}, charged electricity: 0.2 C cm^{-2}, (○) no additive; (●) SnI_2: 100 ppm; (△) SnI_2 200 ppm.

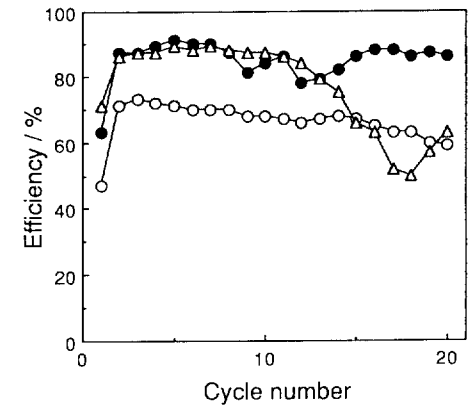

Fig 5 Effect of the addition of AlI_3 on the charge/discharge coulombic efficiency of Li in PC + DME/$LiClO_4$; current density. 2.0 mA cm^{-2}; charged electricity: 0.2 C cm^{-2}, (○) no additive; (●) AlI_3: 100 ppm; (△) AlI_3 200 ppm.

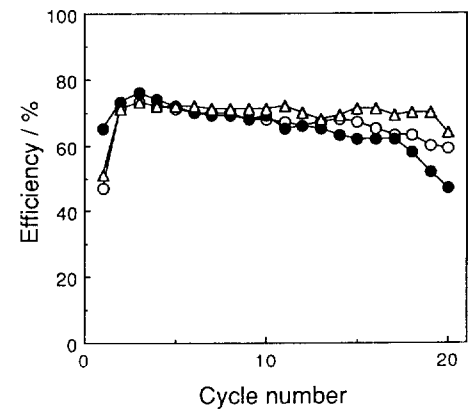

Fig. 6. Effect of the addition of SnI_2 on the charge/discharge coulombic efficiency of Li in PC + DME/$LiClO_4$; current density: 2.0 mA cm^{-2}; charged electricity 0.2 C cm^{-2}, (○) no additive; (●) SnI_2: 100 ppm; (△) SnI_2: 200 ppm.

AlI_3 at the interface [4]. This high resistance is undesirable for the Li cycling with high efficiency. Thus, it is supposed that the addition of SnI_2 did not improve the coulombic efficiency in the present binary electrolyte systems, even if the addition of SnI_2 caused the formation of Li alloy films. Judging from the previous and present results [4], AlI_3 is regarded as a more practical additive than SnI_2 because AlI_3 works effectively under various conditions. The iodide anion may also play an important role in the improvement of the efficiency [4,7]. The effect of the addition of the I^- anion would be ascribed to the physical adsorption of the I^- anion on the electrode. This adsorption would inhibit an interfacial reaction, which forms low-conductive film, between Li and solvents on the Li surface, and hence the cycling behavior of the Li electrode was improved [4,7]. Furthermore, the reaction between the iodide anion and Li on the electrode surface may form a high-conductive LiI layer which prevents the reaction between Li and the solvents. This process may also improve the cycling efficiency of the Li electrode [4,7].

In order to obtain in situ interfacial information, the modified SVET was applied to the detection of the two-dimensional distribution of Li ionic currents on the Li-deposited electrode surface. The potential gradient map of Li-deposited Ni electrode in PC + 2Me-THF/$LiClO_4$ (1.0 mol dm^{-3}) in the absence of the additives during discharge at 25 mV versus Li/Li^+ is shown in Fig. 7. The positive potential gradients corresponding to the anodic ionic currents were observed. However, there was a considerable irregularity of the Li ionic currents on the Ni electrode surface, suggesting that the electrode had many inactive sites for Li stripping. In other words, irregular (dendritic) deposition of Li predominantly proceeded during charging process in the absence of the additives. On the other hand, on the Li-deposited Ni electrode in PC + 2Me-THF/$LiClO_4$ containing AlI_3 (200 ppm) during discharge at 25 mV versus Li/Li^+, the Li ionic currents were very regular in comparison with the non-additive system as shown in Fig. 8. This result suggests that AlI_3 provides anodic stripping of Li with high efficiency over the electrode surface because of the presence of the Li–Al alloy interface with high conductivity. The bias level of the potential gradient (corresponding to the potential gradient value of the bare Ni electrode) varied with each measurement, while the bias level was uniform over the bare Ni electrode surface for each measurement. Unfortunately, therefore, the relative comparison of the magnitude of the potential gradient level cannot be discussed. Fig. 9 shows the potential gradient map of the Li-deposited Ni electrode in PC + 2Me-THF/$LiClO_4$ (1.0 mol dm^{-3}) in the presence of SnI_2 (100 ppm) during discharge at 25 mV versus Li/Li^+. The Li ionic currents in this system were irregular in comparison with the system with AlI_3 especially in the vicinity of x-axis, although they were more regular than the non-additive system probably because of the Sn–Li alloy formation. As described above, the conductivity of the Sn–Li alloy may be low [4]. Therefore, the Li ionic current may converge on the relatively low resistance part (corresponding to the region of a thin Sn–Li alloy layer) of the electrode surface during discharging. This phenomenon would decrease the utility of the overall Li during discharging, resulting in low cycling efficiency.

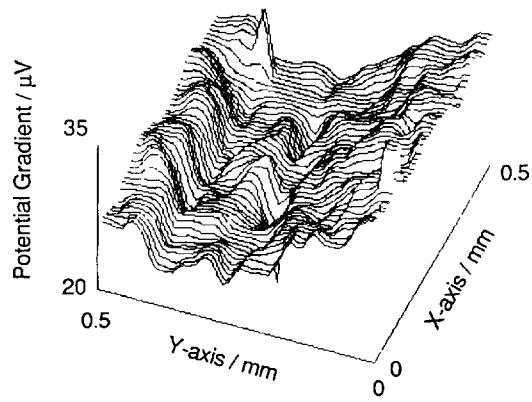

Fig. 7. Potential gradient map of the Li-charged Ni substrate (x–y plane) in PC + 2Me-THF/$LiClO_4$ (1 mol dm^{-3}) during discharge; current density for charge: 2 mA cm^{-2}; charged electricity: 0.2 C cm^{-2}; discharge potential: 25 mV vs Li/Li^+

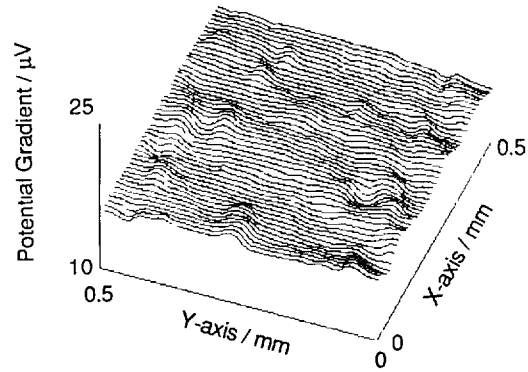

Fig 8 Potential gradient map of the Li-charged Ni substrate (x–y plane) in PC + 2Me-THF/$LiClO_4$ (1 mol dm^{-3}) containing AlI_3 (200 ppm) during discharge; current density for charge 2 mA cm^{-2}; charged electricity, 0.2 C cm^{-2}; discharge potential 25 mV vs Li/Li^+.

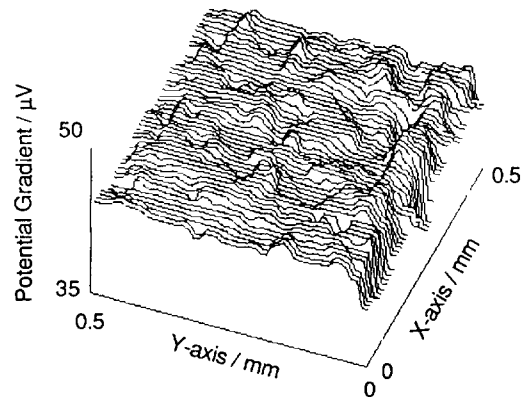

Fig. 9. Potential gradient map of the Li-charged Ni substrate (x–y plane) in PC + 2Me-THF/$LiClO_4$ (1 mol dm^{-3}) containing SnI_2 (100 ppm) during discharge; current density for charge: 2 mA cm^{-2}, charged electricity: 0.2 C cm^{-2}; discharge potential: 25 mV vs. Li/Li^+.

The information of dynamic behavior of the Li ionic current offered by SVET would be useful for the research of advanced Li battery systems, because SVET provides the

clear picture of the distribution of the ionic currents on the electrode.

Acknowledgements

We are grateful to Hokuto Denko Corporation for technical services.

References

[1] J.G. Thevenin and R.H. Muller, *J. Electrochem. Soc., 134* (1987) 273.
[2] D. Aubach, A. Zaban, Y. Gofer, O. Abramson and M. Ben-Zion, *J. Electrochem. Soc., 142* (1995) 687.
[3] N. Takami, T Ohsaki and K Inada, *J. Electrochem Soc., 139* (1992) 1849
[4] Y. Matsuda, M. Ishikawa, S. Yoshitake and M. Morita, *J. Power Sources, 54* (1995) 301.
[5] K. Kanamura, H. Tamura, S. Shiraishi and Z. Takehara, *J. Electrochem. Soc., 142* (1995) 340.
[6] T. Fujieda, N. Yamamoto, K. Saito, T. Ishibashi, M. Honjo, S. Koike, N. Wakabayashi and S. Higuchi, *J. Power Sources, 52* (1994) 197
[7] M. Ishikawa, S. Yoshitake, M. Morita and Y. Matsuda, *J Electrochem. Soc., 141* (1994) L159
[8] Y. Matsuda, *J. Power Sources, 43/44* (1993) 1.